

Article

The Pyrolysis Behaviors of Blended Pellets of Pine Wood and Urea-Formaldehyde Resin

Xiaoteng Li, Siyi Luo *, Zongliang Zuo *, Weiwei Zhang and Dongdong Ren 

School of Environmental and Municipal Engineering, Qingdao University of Technology, 777 Jialingjiang Rd., Qingdao 266033, China

* Correspondence: luosiyi666@126.com (S.L.); zuozongliangneu@163.com (Z.Z.)

Abstract: TG-FTIR and PY-GC/MS were used to analyze the pyrolysis behaviors of pine wood, urea-formaldehyde resin (UF resin) and their blended pellets. The pyrolysis process was divided into three stages: water evaporation, devolatilization and pyrolysis residue decomposition. During the pyrolysis process of the blended pellets, with the increase of the addition ratio of UF resin, the peak value of the weight loss decreased in the decomposition stage of the pyrolysis residue, while the temperature shifted to the low-temperature region. This was mainly due to the structural stability of pyrolytic carbon produced by UF resin, which hindered the thermal decomposition of lignin-produced residues in pine. FTIR showed that CO₂ was the main product of pyrolysis. For UF resin, nitrogen compounds accounted for a large proportion. With the addition of UF resin, the nitrogen in the blended pellets increased significantly. Since the synergistic effect promoted the further decomposition of the organic oxygen-containing structure, the NO release was still increased. PY-GC/MS showed that co-pyrolysis produced more nitrogen-containing compounds and promoted the decomposition of macromolecular phenol derivatives, lipids and ketones, resulting in more small-molecule acids and alcohols.

Keywords: pyrolysis; pine wood; urea-formaldehyde resin



Citation: Li, X.; Luo, S.; Zuo, Z.; Zhang, W.; Ren, D. The Pyrolysis Behaviors of Blended Pellets of Pine Wood and Urea-Formaldehyde Resin. *Energies* **2023**, *16*, 2049. <https://doi.org/10.3390/en16042049>

Academic Editor: Dino Musmarra

Received: 23 November 2022

Revised: 5 January 2023

Accepted: 23 January 2023

Published: 19 February 2023



Copyright: © 2023 by the authors. Licensee MDPI, Basel, Switzerland. This article is an open access article distributed under the terms and conditions of the Creative Commons Attribution (CC BY) license (<https://creativecommons.org/licenses/by/4.0/>).

1. Introduction

Plywood is the earliest wood-based panel developed but also the type of wood-based panel with the largest output in China. It is made of artificial fast-growing poplar, eucalyptus, pine, fir and bamboo as the main raw materials and is pressed by adding adhesive [1]. With the rapid development of China's wood industry, the emergence of adhesives not only plays a positive role in saving wood products raw materials and simplifying wood products processing technology but also promotes the sustained growth of China's economy to a certain extent [2]. UF resin adhesive is the most widely used synthetic resin adhesive in China's wood industry because of its advantages of abundant raw materials, low production cost and fast curing speed [3]. However, at the same time, a large number of discarded wood-based panels and their products pose a threat to the environment. Using traditional treatment methods such as incineration and burial will not only waste wood resources [4] but a large amount of nitrogen contained in UF resin will also be converted into dioxins, NO_x and other pollutants, causing serious harm to the environment.

In order to effectively avoid the environmental pollution and resource waste caused by the traditional treatment of waste wood-based panels and create considerable economic value [4], many researchers have conducted research on the recycling and reuse of waste wood-based panels. Lykidis et al. treated particleboard by the hydrothermal method, which reduces the amount of formaldehyde released, but the method is inefficient and time-consuming [5]. In view of the disadvantages of the hydrothermal method, Zhang [6] chose steam the explosion method to treat particleboard. It was found that steam explosion

can effectively remove most of the UF resin in the particleboard and, at the same time, reduce the formaldehyde content in the recycled particleboard, which was helpful for the reduction of the formaldehyde content in later products; however, with the increase of the blasting pressure, the cell structure of wood will be further destroyed. Pyrolysis can convert particleboard into biomass fuel with a high calorific value, replacing some traditional fossil fuels for an energy supply [7]. Park et al. [8] conducted co-pyrolysis of polypropylene and discarded wood-based panels in an intermittent reactor. The results showed that the co-pyrolysis of plastic and plywood can increase the yield of wood tar, reduce the generation of oxides and water and improve the product quality of liquid fuel. Pierre Girods [9,10] adopted “two-step pyrolysis” to process particleboard, which reduces the interference of the N element on biomass pyrolysis and prevents the formation of dangerous compounds such as NO₂. It has also been found that the adsorption capacity of activated carbon from wood-based panel pyrolysis to phenol in wastewater is better than that from biomass pyrolysis. However, there have been few studies on the interaction between UF resin and biomass by changing the ratio of them in the pyrolysis process.

Recycling waste wood-based panels into high-performance materials has also become one of the current research trends. Lu Jun et al. [11] hot-pressed phenolic resin and waste wood-based panels into a composite material, and the flame retardancy of the new composite material was significantly higher than that of MDF. Fang Hongxia et al. [12] modified bamboo fiber material with phenolic resin, and the thermal stability of the composite material was increased.

In this study, TG-FTIR and PY-GC/MS are used to analyze the pyrolysis and products' distribution characteristics of blended pellets with different proportions of pine and UF resin. The effect of the introduction of UF resin on the pellets' pyrolysis and the synergistic mechanism are investigated. The results are helpful to better understand the pyrolysis behavior of blended pellets and provide theoretical guidance for industrial waste particleboard disposal.

2. Materials and Methods

2.1. Materials

The UF resin was obtained from the waste wood-based panels produced by a building decoration company in Jinan City, Shandong Province, China. Pine wood (PW) was obtained from Shijiazhuang City, Hebei Province, China. The samples were crushed to less than 74 μm before the tests and then put in an oven at 105 °C for 24 h to remove moisture. The industrial analysis and elemental analysis are presented in Table 1. The final samples were pressurized pelletizing by the mixing of PW and UF resin, with the mass ratios, respectively, being 1:0, 5:1, 2:1 and 0:1.

Table 1. Elemental analysis and industrial analysis of the samples.

	Elemental Analysis (wt%)					Industrial Analysis (wt%)			
	C	H	O ¹	N	S	M	V	A	FC
UF resin	33.65	5.46	32.23	17.50	0	9.78	74.17	1.38	14.67
PW	33.25	4.52	24.27	0.90	0.29	5.28	56.84	31.49	6.39
Chlorella Vulgaris [13]	49.71	7.21	24.66	8.75	0.54	1.89	75.42	9.13	13.56
Rice husk [13]	40.10	5.09	40.93	0.44	0	11.23	66.74	13.44	8.59
Moso Bamboo [14]	44.87	5.73	38.32	0.71	0.01	8.67	74.81	2.56	13.96
Eucalyptus Dunnii [15]	45.67	6.50	46.74	0.14	0.96	4.37	84.86	0.31	14.83

¹O(wt%) = 100%-C-H-N-S-M-A; FC = 100%-M-V-A.

By comparing with other biomass, UF resin contains more nitrogen and a higher fixed carbon content.

2.2. Pellet Preparation Experiment

According to the experimental setups and methods from the literature [16], take about 4 g of raw material and put it into the designated ball mold, keep it under constant pressure for ten minutes, press the molding and take it out. Prepared blended pellets of different proportions (PW and PW:UF = 5:1, PW:UF = 2:1, UF resin) for subsequent experiments.

2.3. TG-FTIR

About 1 g of sample from each proportion of pellets was used in TG-FTIR. Under a flow of helium (99.9%) at 50 mL/min, samples were heated from 25 °C to 800 °C at an increase of 20 °C/min and analyzed using a thermogravimetric analyzer (NETZSCH 209F3, Germany, Netzsch Company). Gas produced by pyrolysis was detected using an infrared spectrometer (SENSOR 27 Bruker, Tianjin, Golden Bell Technology Co., Ltd.). Data was obtained by averaging 16 scans with a resolution of 4 cm⁻¹ within the wavenumber range of 4000 to 399 cm⁻¹ and was processed using OMNIC 8.0 software (Thermo Nicolet, USA).

2.4. PY-GC/MS

The pyrolytic volatiles were measured and identified using gas chromatography/mass spectrometry. For the pyrolysis stage, a 10 mg sample was pyrolyzed at 450 °C for 24 s by using a pyrolysis reactor (Frontier EGA/PY-3030D, Japan, Louie Enterprises Limited) with helium as the carrier gas (0.8 mL/min). Volatiles were separated with a capillary column DP-5MS Agilent 19091S-433 (0.25 mm × 30 m × 0.25 μm) using the following temperature program: start at 50 °C and hold for 1 min, ramp at 10 °C/min to 300 °C and hold for 1 min. The yield of the compound was calculated using GC-MS spectra based on standard solution calibration and the NIST database (NIST 107).

2.5. The Interaction Effect of Co-Pyrolysis

ΔW was introduced to evaluate the synergistic effect of UF resin and PW co-pyrolysis, which represented the deviation of the theoretical values from the experimental ones. The formula was as follows [17]:

$$\Delta W = W_{\text{exptl}} - W_{\text{calcd}} \quad (1)$$

where ΔW represented the experimental weight loss value of the blend, W_{exptl} indicated the actual weight loss value of the co-pyrolysis of UF resin and PW and W_{calcd} was the theoretical weight loss value calculated from the independent sample weight loss value. Its calculation formula was:

$$W_{\text{calcd}} = X_T W_T + X_C W_C \quad (2)$$

X_T and X_C refer to the mass ratio of UF resin and PW in the blended pellet, respectively, and W_T and W_C were the weight loss of urea-formaldehyde resin and pine wood during individual pyrolysis conditions. $\Delta W > 0$ indicated that co-pyrolysis has a promoting effect, which was defined as a positive synergistic effect, and $\Delta W < 0$ indicated that there is an inhibiting effect [18].

3. Results and Discussion

3.1. Effect of the Introduction of UF Resin on the Pyrolysis Characteristics of Blended Pellets

3.1.1. Pyrolysis Characteristics of PW Pellets

From Figure 1a, it can be seen that the pyrolysis process of PW pellets is divided into three stages. The first stage (3.32% weight loss) is attributed to the dehydration and drying from room temperature to 157 °C, mainly including the removal of bound water and free water in PW. It can be seen from the DTG curve that the weight loss is small at this stage. The second stage is the devolatilization stage from 157 °C to 460 °C, which is mainly related to the thermal decomposition of cellulose, hemicellulose and lignin. This is because the decomposition temperature range of hemicellulose is 225–350 °C, 325–375 °C for cellulose and 250–500 °C for lignin [19]. It can be seen from the DTG curve that there are two weight loss peaks (303 °C and 343 °C) at this stage, mainly corresponding to the largest weight

loss peaks of hemicellulose and cellulose. The third stage is the decomposition process of the pyrolysis residue. The PW pellet has an obvious weight loss process at this stage, which is mainly due to the further cracking process of the PW residues decomposed by lignin, and reaches the maximum weight loss rate at 765 °C.

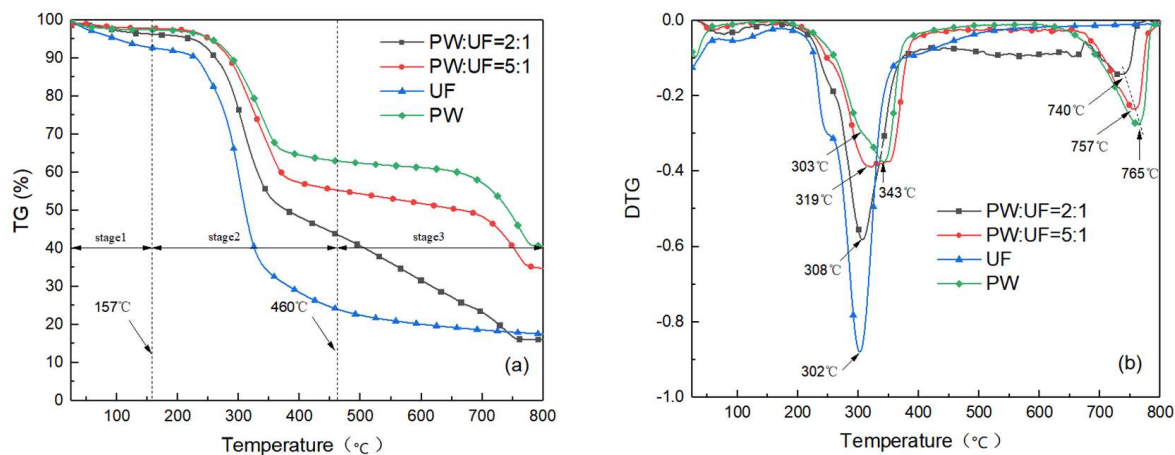


Figure 1. TG and DTG curves of pyrolysis. ((a) TG curves; (b) DTG curves).

3.1.2. Pyrolysis Characteristics of UF Resin Pellets

For UF resin pellets, the first stage is the water evaporation and free formaldehyde release stage [20]. Similar to PW, weight loss is slow at this stage. The second stage (66% weight loss) is the devolatilization stage, which is mainly due to the weight loss caused by the breaking of a large number of chemical bonds. The hydroxymethyl group is split to form formaldehyde, the C-N bond is broken and volatile substances are generated [21]. The TG curve presents that the thermal stability of UF resin is lower than that of PW, and the maximum weight loss peak (302 °C) is reached at a lower temperature, mainly because the thermal stability of UF resin is worse than that of PW. The third stage is mainly the decomposition process of the pyrolysis residue. The mass is almost unchanged, and the structure of the residual material tends to be stable.

3.1.3. Effect of UF Resin on Pyrolysis Characteristics of Blended Pellets

For the blended pellets, the main pyrolysis process is similar to that of PW. Both the second stage and the third stage have obvious weight loss processes. The TG curve shifts markedly to the low-temperature region after adding UF resin. According to the DTG curve, the maximum weight loss rate of the blended pellets at the devolatilization stage is greater than that of the PW pellets, and at the same time, the weightless peak moves to the low-temperature region. In the third stage, with the increase of the proportion of UF resin added, the peak value of the weight loss peak becomes smaller, and the required temperature becomes lower at the same time. The main reason may be that the pyrolytic carbon produced by UF resin is stable in structure, which inhibits the thermal decomposition of lignin-generated residues in PW.

According to Figure 2, there is an obvious deviation between the experimental value and theoretical value of UF resin and PW-blended pellets. When the temperature is lower than 285 °C, $\Delta W < 0$, which is due to the small molecules in the UF resin and PW beginning to decompose, and there is an inhibitory effect between the UF resin and PW. The inhibitory effect decreases as the proportion of UF resin increases. As the addition ratio of the UF resin increases, the temperature at $\Delta W = 0$ shifts slightly to the low-temperature region. When the temperature is higher than 286 °C, ΔW begins to move forward and shows a sharp increasing trend, indicating that there is an obvious positive synergy between the UF resin and PW until the end of the reaction. Between 286 °C and 400 °C, the synergistic effect increases with the increase of the proportion of UF resin, but the opposite effect is observed after 400 °C. It is because the urea-formaldehyde resin basically completes the

pyrolysis at 400 °C, and the generated pyrolytic carbon has a stable structure and is not easy to decompose again.

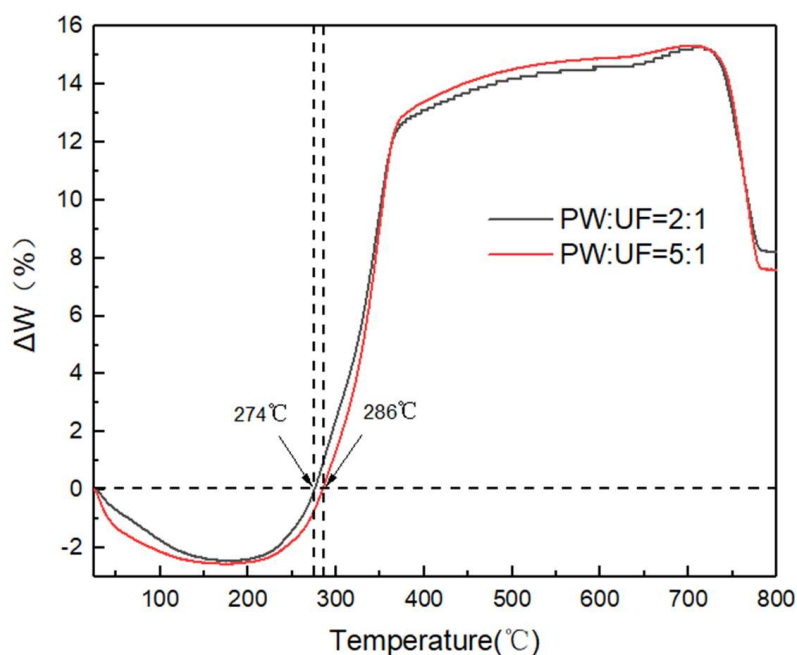


Figure 2. ΔW of blended pellets with different proportions.

3.2. Gas Phase Product Analysis of Pyrolysis

Figure 3 shows the three-dimensional infrared spectra of pyrolytic gases of four samples detected by FTIR in nitrogen atmosphere. Through the wavenumber and intensity of the absorption band in the three-dimensional infrared spectrum, the variation trend of the gas species and the amount released during the pyrolysis process with the pyrolysis temperature can be qualitatively analyzed. The infrared characteristic absorption wave number (unity: cm^{-1}) is the most obvious at 669 and 2358 cm^{-1} , indicating that CO_2 is a major product of sample pyrolysis. At the same time, it can be seen that the temperature range of pyrolysis gas released from the PW pellets is mainly concentrated in 200~350 °C and 600~750 °C. The pyrolysis gas release of the UF resin pellet is mainly concentrated at 180~350 °C. for the mixed pellet, and the results are more complicated due to the interaction between UF resin and PW during the pyrolysis process.

The infrared spectra of pyrolysis gaseous products at the maximum weight loss peak of different samples are shown in Figure 4. It can be observed that the main functional groups are H_2O (4000–3500 cm^{-1}), CH_4 (3115–2675 cm^{-1}), CO_2 (2400–2240, 680–660 cm^{-1}), CO (2240–2060 cm^{-1}), $\text{C}=\text{O}$ (1900–1600 cm^{-1}), $\text{C}-\text{O}$ and $\text{C}-\text{H}$ (1600–1450 and 1300–1200 cm^{-1}) and NH_3 (966 cm^{-1}) [22].

In order to empathize the pyrolysis mechanism of blended pellets, a study was carried out on the release trend of the main gas products with real-time temperature changes. The evolution characteristics of pyrolysis gas with temperature changes are shown in Figure 5. For the pyrolysis of PW pellets, it is found that all gas products reach the maximum at the maximum weight loss rate, except for CO_2 , which has two peaks, while all other products have one peak. CO_2 is mainly produced by decarboxylation and decarbonylation reactions and the secondary cracking of solid-phase coking resulting in chain scission and reforming reactions [22,23]. The methoxy group of the weak bond and the methylene group with higher bond energy are cleaved to produce CH_4 [24]. H_2O is mainly generated by bulk water, bound water, crystal water in the sample and the cleavage of oxygen functional groups during the pyrolysis process [25]. The remaining gas products are less.

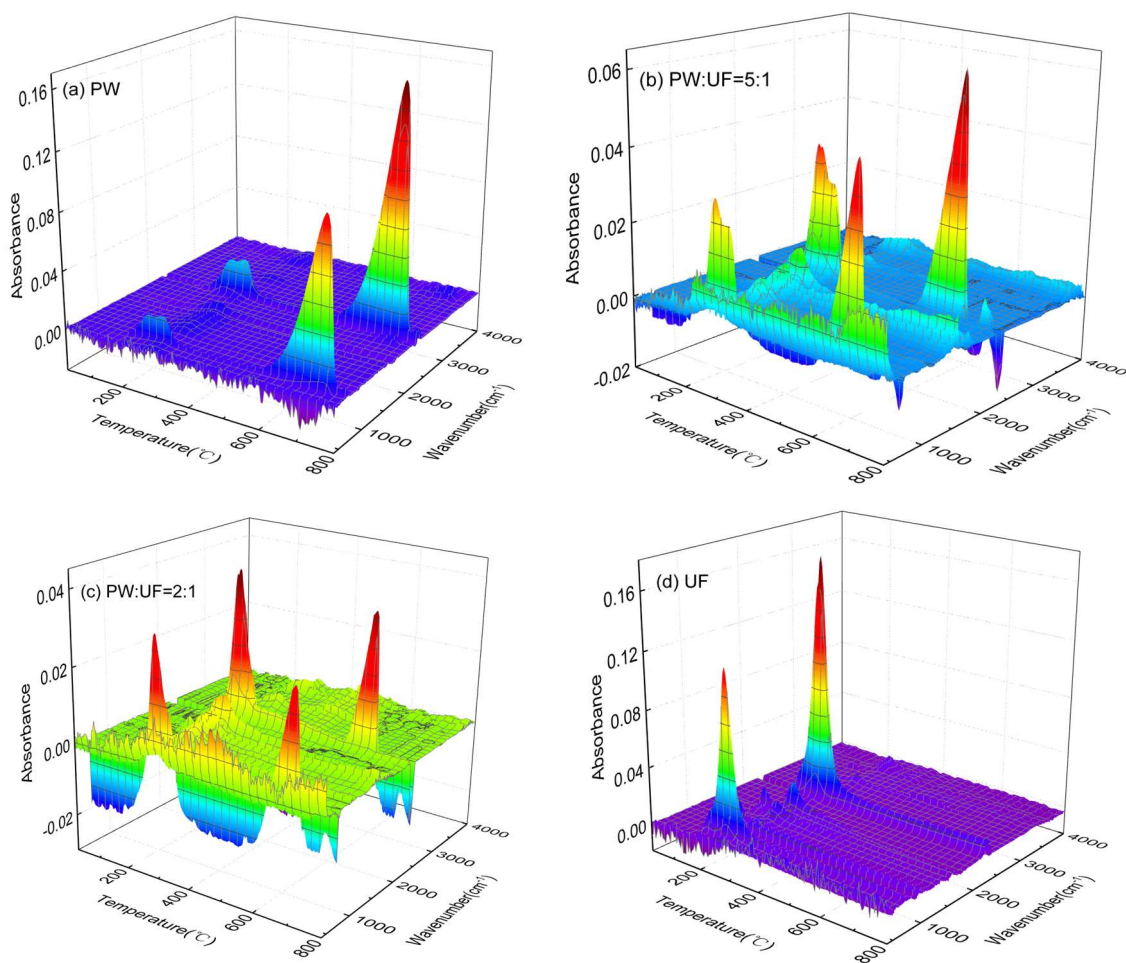


Figure 3. Three—dimensional infrared spectrogram. ((a) PW, (b) PW:UF = 5:1, (c) PW:UF = 2:1 and (d) UF).

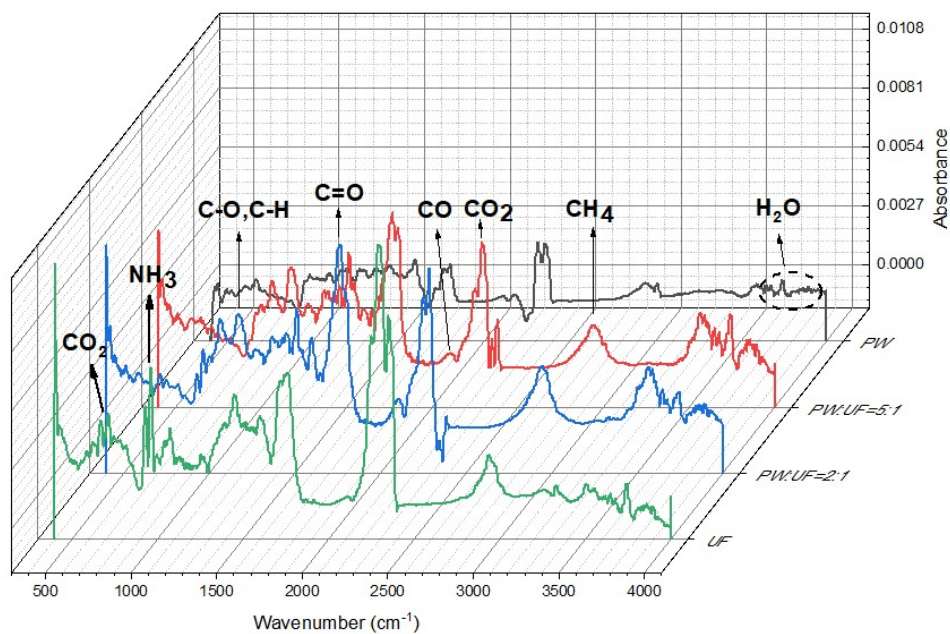


Figure 4. FTIR spectra of gaseous products obtained at the maximum weight loss peak.

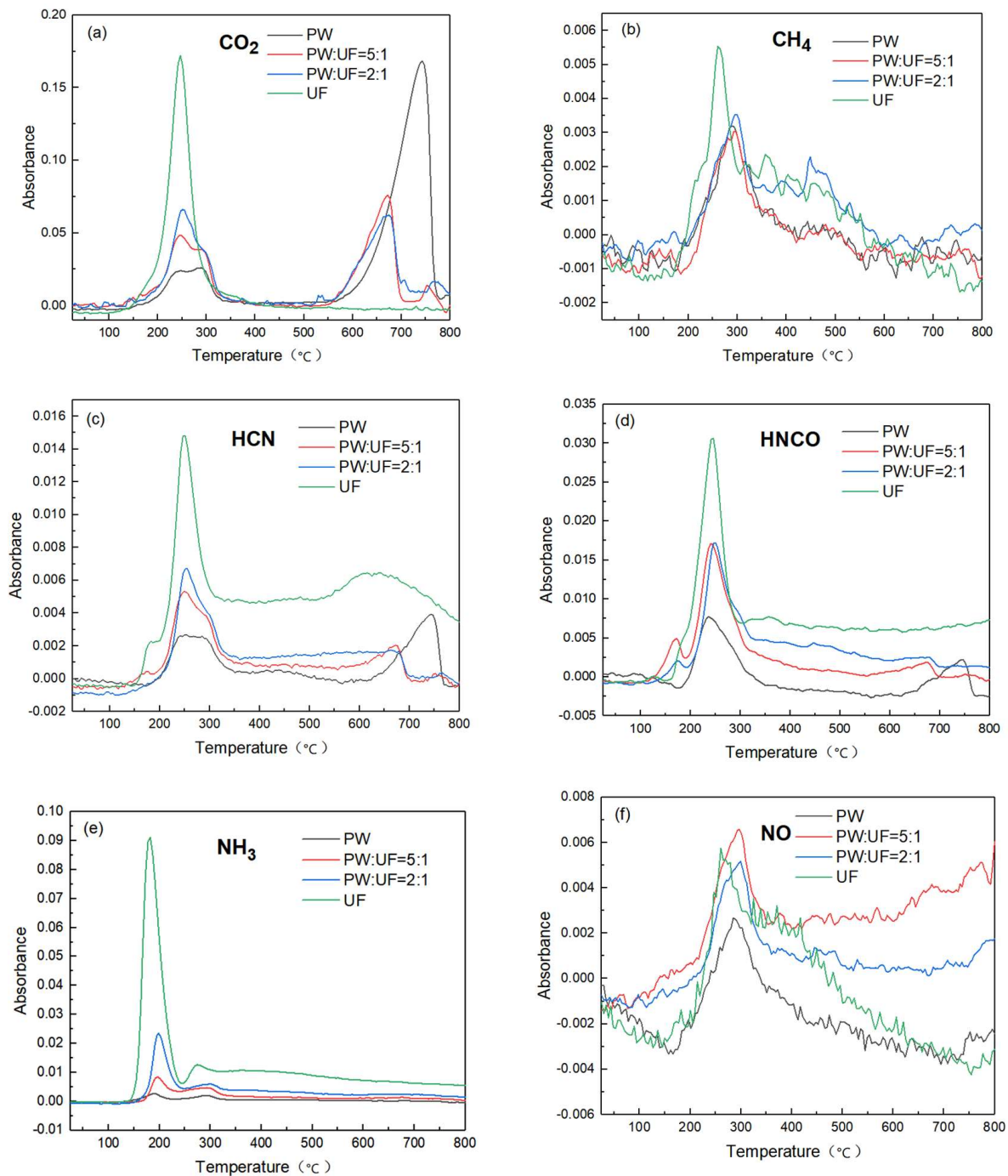


Figure 5. The evolution characteristics of main gas products as a function of the temperature. (a) CO₂; (b) CH₄; (c) HCN; (d) HNCO; (e) NH₃; (f) NO.

Different with PW, the pyrolysis of UF resin pellets mainly produces CO₂, CH₄, HCN, HNCO and NH₃. CO₂ is mainly formed by the rapid decomposition of a large amount of R-CHO, R-COOH, R-OH and C_xH_y generated during the pyrolysis of UF resin pellets. CH₄ is mainly produced by the further pyrolysis of R-COOH, R-CHO, R-COO-R group macromolecules and C_xH_y in UF resin [26]. Due to the high nitrogen content of UF resin, nitrogen compounds occupy a large part of the product. NH₃, the second-largest product after CO₂, is produced at 150 °C and reaches its maximum absorbance at 180 °C. HNCO is produced at 160 °C and reaches its maximum absorbance at 245 °C. The temperature at which NH₃ and HNCO reach the maximum absorbance is lower than the temperature

required for the maximum weight loss rate of UF resin. This result indicates that nitrogen is removed from UF resin at lower temperatures, which is consistent with former studies [27]. H₂O is mainly generated from the separation of free water and the rupture of molecular bonds in UF resin.

In addition, it can also be observed that the effects of UF resin on the pyrolysis gas composition are mainly reflected in the nitrogen-containing compounds during pyrolysis. The nitrogen content of PW is very low, and the production trend of HCN, HNCO and NH₃ is similar to that of UF resin, and the maximum absorption peaks of HCN, HNCO and NH₃ are significantly increased compared with PW. The temperature required for the second absorption peak of CO₂ decreases dramatically, mainly due to UF resin promoting the decomposition of solid-phase coking in PW. With the addition of UF resin, the production trend of NO increased greatly, which is much higher than that of UF resin and PW pyrolysis alone; it is possible that the co-pyrolysis of UF resin and PW promotes the further decomposition of the organic oxygen-containing structure, which improves the release of NO.

3.3. Compositional Analysis of Liquid Phase Products of Co-Pyrolysis

To investigate the formation of the main product components during individual pyrolysis and co-pyrolysis, samples are analyzed by gas chromatography-mass spectrometry (PY-GC/MS). A tentative identification of the volatile compounds present is achieved by comparing the observed mass spectra with the data system library (NIST) and published spectra supported by retention index data, which are then compared against the available literature listing known retention indices. The chemical compositions of the sample pyrolysis products are shown in Table 2.

Table 2. Chemical composition analysis results of the sample pyrolysis products.

Number	m/z	Molecular Formula	Compound Name	Area (%)			
				PW	PW:UF = 5:1	PW:UF = 2:1	UF resin
1	180	C ₁₀ H ₁₂ O ₃	Phenol,2,6-dimethoxy-4-vinyl-	6.83	7.56	6.87	-
2	180	C ₁₀ H ₁₂ O ₃	4-((1E)-3-Hydroxy-1-propenyl)-2-methoxyphenol	6.54	4.02	3.09	-
3	60	C ₂ H ₄ O ₂	Acetic acid	4.77	5.25	3.92	0.82
4	154	C ₈ H ₁₀ O ₃	2,6-Dimethoxyphenol	4.71	6.02	5.33	-
5	89	C ₃ H ₇ NO ₂	Sarcosine	4.66	8.81	10.91	17.27
6	194	C ₁₁ H ₁₄ O ₃	€-2,6-Dimethoxy-4-(prop-1-en-1-yl)phenol	4.6	5.52	4.93	-
7	210	C ₁₁ H ₁₄ O ₄	trans-Sinapyl alcohol	4.01	1.16	0.74	-
8	150	C ₉ H ₁₀ O ₂	4-Hydroxy-3-methoxystyrene	3.24	3.72	3.26	-
9	74	C ₃ H ₆ O ₂	Hydroxyacetone	2.95	2.03	1.62	-
10	86	C ₄ H ₆ O ₂	Butanedial	2.62	-	-	-
11	113	C ₄ H ₇ N ₃ O	Creatinine	2.48	-	-	-
12	98	C ₅ H ₆ O ₂	1,2-Cyclopentanedione	2.31	2.67	1.87	-
13	168	C ₉ H ₁₂ O ₃	Phenol,2,6-dimethoxy-4-methyl-	2.24	2.51	2.01	-
14	124	C ₇ H ₈ O ₂	Guaiacol	2.14	2.64	2.1	-
15	164	C ₁₀ H ₁₂	€(e)-isoeugenol	2.09	2.64	2.27	-
16	72	C ₄ H ₈ O	Cyclopropyl carbinol	2.03	-	1.86	-
17	94	C ₆ H ₆ O	Phenol	1.99	2.08	2.04	-
18	104	C ₄ H ₈ O ₃	1,2-Ethanediol,1-acetate	1.91	-	-	-
19	130	C ₄ H ₃ FN ₂ O ₂	5-Fluorouracil	1.62	1.06	0.77	-
20	138	C ₈ H ₁₀ O ₂	2-Methoxy-4-methylphenol	1.53	1.07	0.95	-
21	194	C ₁₁ H ₁₄ O ₃	Phenol,2,6-dimethoxy-4-(2-propen-1-yl)-	1.35	1.5	1.93	-
22	210	C ₁₁ H ₁₄ O ₄	2-Propanone,1-(4-hydroxy-3,5-dimethoxyphenyl)-	1.14	0.76	0.74	-
23	317	C ₂₀ H ₁₅ NO ₃	Benzoic acid, 2-[[[1,1'-biphenyl]-4-ylamino] carbonyl]-	-	-	-	9.39

Table 2. Cont.

Number	<i>m/z</i>	Molecular Formula	Compound Name	Area (%)			
				PW	PW:UF = 5:1	PW:UF = 2:1	UF resin
24	162	C ₆ H ₁₀ O ₅	1,6-anhydro-beta-d-glucopyranos	5.98	1.25	2.08	-
25	102	C ₄ H ₆ O ₃	Methyl pyruvate	-	1.88	1.97	5.84
26	144	C ₆ H ₈ O ₄	1,4:3,6-Dianhydro- α -D-glucopyranose	0.42	-	-	3.45
27	98	C ₅ H ₆ O ₂	3-Furanmethanol	-	-	-	2.7
28	71	C ₄ H ₉ N	Cyclobutylamine	-	-	-	2.58
29	84	C ₄ H ₈ N ₂	N, N-Dimethylglycinonitrile	-	-	-	2.4
30	128	C ₈ H ₁₆ O	2,2-Dimethylcyclohexanol	-	-	-	2.33
31	129	C ₆ H ₁₅ N ₃	hexahydro-1,3,5-trimethyl-s-triazin	-	-	-	2.17
32	112	C ₆ H ₈ O ₂	Methyl cyclopentenolone	-	-	-	1.68
33	109	C ₆ H ₇ NO	2-Acetyl pyrrole	-	-	-	1.58
34	134	C ₉ H ₁₀ O	Phenylacetone	-	-	-	1.38
35	256	C ₁₆ H ₃₂ O ₂	Palmitic acid	-	0.41	0.49	1.35
36	128	C ₆ H ₁₂ N ₂ O	5-Amino-1-methyl-2-piperidinone	-	0.36	0.46	1.15
37	88	C ₄ H ₁₂ N ₂	1,3-Propanediamine, N1-methyl-	-	1.93	-	-
38	164	C ₁₀ H ₁₂ O ₂	Phenol,2-methoxy-4-(1-propen-1-yl)-	-	1.65	-	-
39	238	C ₁₅ H ₂₆ O ₂	3-methyl-, 3,7-dimethyl-2,6-octadienyl ester, (E)-Butanoic acid	0.01	1.2	0.06	-
40	362	C ₁₈ H ₂₂ N ₂ O ₄ S	Thiazolidine-2,4-dione, 5-(2-methoxybenzylidene)-3-(2,6-dimethylmorpholinomethyl)-	-	-	3.06	-
41	112	C ₆ H ₈ O ₂	3-Methyl-1,2-cyclopentanedione	1.02	1.86	1.98	-
42	84	C ₄ H ₄ O ₂	2(5H)-Furanone	1.15	1.55	1.73	1.97
43	98	C ₅ H ₆ O ₂	Furfuryl alcohol	0.79	1.06	1.24	-
44	198	C ₈ H ₁₈ N ₆	2,2'-Azobis-2-methylpropanimidamide	0.08	1.28	1.21	0.08
45	152	C ₉ H ₁₂ O ₂	4-Ethyl-2-methoxyphenol	0.58	1.12	1.12	-

For the pyrolysis products of PW, 30 main absorption peaks are detected; these volatiles are divided into esters, aldehydes, alcohols, fatty acids, ketones and furan based on their chemical nature. The proportions of others are Phenol-2,6-dimethoxy-4-vinyl- (6.83%), Acetic acid (4.77%), 4-((1E)-3-Hydroxy-1-propenyl)-2-methoxyphenol (6.54%), 2,6-Dimethoxyphenol (4.71%), Sarcosine (4.66%), 1,6-anhydro-beta-d-glucopyranos (5.98%), (E)-2,6-Dimethoxy-4-(prop-1-en-1-yl) phenol (4.60%), trans-Sinapyl alcohol (4.01%), 4-Hydroxy-3-methoxystyrene (3.24%), Hydroxyacetone (2.95%), butanedial (2.62%) and creatinine (2.48%). Phenolic compounds account for the largest proportion of all products, mainly from the decomposition of lignin [28]. The main structural units of lignin are ether bonds (β -O-4, α -O-4, 4-O-5 and 5-O-4) and carbon-carbon bonds (β -5, β - β and 5-5) [29]. Due to the small bond energy, ether bonds are easier to break than carbon-carbon bonds, thereby releasing volatile phenolic compounds [29]. Acetic acid is mainly produced by the elimination of the acetyl group attached to the xylose unit [30]; at the same time, in the early stage of hemicellulose decomposition, 4-methyl-d-glucuronic acid-base cleavage and the cleavage of the carboxyl group will produce acetic acid [28]. In addition, the ring-opening reaction of cellulose and the cleavage reaction of the lignin side chain also produce acetic acid [31,32]. Through the literature review, it is found that various dehydrated sugar products and derivatives are formed through the depolymerization of cellulose and hemicellulose at the initial stage of pyrolysis [33]. At the same time, the cleavage of grape-mannan, which is relatively high in PW, also produces dehydrated sugars [29]. As the pyrolysis progressed, the small molecule aldol compound is obtained by breaking the molecular bond between the glucose monomer C₂ and C₃ and opening the hemiacetal group ring, causing large amounts of glucose to be resolved [34], such as butaraldehyde, 1,2-cyclopentodione, etc. During the pyrolysis of cellulose and hemicellulose, the pyran ring is opened; the acetal reaction occurs to form a furan ring and then a variety of furan products are generated [35], such as 2(5H)-furanone, furfuryl alcohol and so on.

The product components of UF resin pyrolysis alone are simpler than PW. Mainly including sarcosine (17.27%), Kartogenin (9.39%), Methyl pyruvate (5.84%), 1,4:3,6-Dianhydro-d-glucopyranose (3.45%), 3-Furanmethanol (2.7%), Cyclobutylamine (2.58%), Dimethylaminoacetonitrile (2.4%), 2,2-Dimethylcyclohexanol (2.33%) and hexahydro-1,3,5-trimethyls-triazin (2.17%). In addition, there are pyrrole, furan compounds produced. It can be found that nitrogen-containing compounds are the main components of UF resin pyrolysis oil.

As can be seen from Table 2, the co-pyrolysis products are more complex than those of PW. With the addition of UF resin, more nitrogenous compounds appeared in the co-pyrolysis solution, such as 1,3-Propanediamine, N1-methyl- and Thiazolidine-2,4-dione,5-(2-methoxybenzylidene)-3-(2,6-dimethylmorpholinomethyl)-,2,2'-Azobis-2- methylpropa-nimidamide. In addition, it can be found that some products of individual pyrolysis were not detected in the co-pyrolysis products, which proved that the co-pyrolysis of PW and UF resin was not a simple superposition effect. The analysis found that the interaction between pine wood and urea-formaldehyde resin promoted the decomposition of macromolecular phenol derivatives, as well as the decomposition of lipids and ketones, resulting in more small molecular acids and alcohols, such as acetic acid, furfuryl alcohol, etc.

4. Conclusions

The pyrolysis behaviors of PW, UF resin and blended pellets were analyzed by TG-FTIR and PY-GC/MS to explore the interaction mechanism. The results showed that the pyrolysis process of the testing samples is divided into three stages: a water evaporation stage, devolatilization stage and pyrolysis residue decomposition stage, and all reached the maximum weight loss rate in the devolatilization stage. The DTG curve showed that the thermal stability of UF resin was lower than that of PW. In the pyrolysis process of the blended pellets, with the increase of the UF resin addition ratio, the peak value of the weight loss peak became smaller in the decomposition stage of pyrolysis residue, and the temperature shifted to the low-temperature region. It was mainly due to the structural stability of pyrolytic carbon produced by UF resin, which hindered the thermal decomposition of lignin-produced residues in PW.

It was found that the effect of UF resin on the pyrolysis of PW was mainly on nitrogen-containing compounds through FTIR. The contents of NH₃, HNCO and HCN in the pyrolysis gas products of the blended pellets increased significantly. The production trend of NO increased significantly, which was higher than that of UF resin and PW individual pyrolysis, probably because the co-pyrolysis of UF resin and PW promoted the further decomposition of the organic oxygen-containing structure, which increased the NO release.

According to the analysis of the results of PY-GC/MS, it can be found that the pyrolysis of blended pellets produces more nitrogen-containing compounds, while co-pyrolysis promoted the decomposition of macromolecular phenol derivatives, as well as the decomposition of lipids and ketones, resulting in more small molecular acids and alcohols.

Author Contributions: Validation, X.L.; Writing—original draft, X.L.; Writing—review & editing, W.Z. and D.R.; Funding acquisition, S.L. and Z.Z. All authors have read and agreed to the published version of the manuscript.

Funding: This research was funded by the National Natural Science Foundation of China (52104397) and the 2020 Science and Technology Project of Qingdao West Coast New Area (2020–99).

Data Availability Statement: Not applicable.

Conflicts of Interest: The authors declare no conflict of interest.

References

1. Xiaobing, X. Status of Wood-based Panel Industry in China. *China Wood Ind.* **2016**, *30*, 11–14+28. [[CrossRef](#)]
2. Renwei, S.; Meifen, T. Application Status of Adhesives in Wood-based Panels. *J. Green Sci. Technol.* **2020**, 139–140. [[CrossRef](#)]
3. Yufeng, M.; Xuanang, G.; Chunpeng, W. Research Progress in Wood Adhesives. *Chem. Ind. For. Prod.* **2020**, *40*, 1–15. [[CrossRef](#)]

4. Tianhang, R.; Ming, L.; Yiqiang, W.; Xingong, L.; Yan, Q. Research Progress on the Recycling of Waste Wood-Based Panels. *China For. Prod. Ind.* **2022**, *59*, 34–40. [[CrossRef](#)]
5. Lykidis, C.; Grigoriou, A. Hydrothermal recycling of waste and performance of the recycled wooden particleboards. *Waste Manag.* **2008**, *28*, 57–63. [[CrossRef](#)]
6. Derong, Z. The Properties of the Regenerated Partcles by Steam Explosion and the Particleboard Manufacture Technology. *J. Beijing For. Univ.* **2010**, *21*, 5—7+23.
7. Meng-meng, S.; Wei-tao, X.; Tong-tong, C.; Hao-yuan, L.; Qi, L. Application of Pretreatment Technology in Biomass Pyrolysis. *China For. Prod. Ind.* **2019**, *46*, 33–38. [[CrossRef](#)]
8. Park, H.J.; Heo, H.S.; Yoo, K.-S.; Yim, J.-H.; Sohn, J.M.; Jeong, K.-E.; Jeon, J.-K.; Park, Y.-K. Thermal degradation of plywood with block polypropylene in TG and batch reactor system. *J. Ind. Eng. Chem.* **2011**, *17*, 549–553. [[CrossRef](#)]
9. Girods, P.; Dufour, A.; Rogaume, Y.; Rogaume, C.; Zoulalian, A. Pyrolysis of wood waste containing urea-formaldehyde and melamine-formaldehyde resins. *J. Anal. Appl. Pyrolysis* **2008**, *81*, 113–120. [[CrossRef](#)]
10. Girods, P.; Dufour, A.; Rogaume, Y.; Rogaume, C.; Zoulalian, A. Comparison of gasification and pyrolysis of thermal pre-treated wood board waste. *J. Anal. Appl. Pyrolysis* **2009**, *85*, 171–183. [[CrossRef](#)]
11. Jun, L. Thermal Analysis on PF/ Waste Medium Density Fiberboard Composite by TG and DSC. *China Wood Ind.* **2015**, *29*, 14–17. [[CrossRef](#)]
12. Fang, H.; Wu, Q.; Jiang, R.; Li, H.; Zheng, Y.; Han, X. Perparation and Carbonization Behavior of Bamboo Fiber Modified by Copolymerized Phenolic Resin. *Chin. J. Mater. Res.* **2014**, *28*, 853–857.
13. Yuqing, X.; Yanfen, L.; Xiaoqian, M.; Na, S. Co-pyrolysis characteristics and kinetics of chlorella vulgaris and rice husk. *Renew. Energy Resour.* **2021**, *39*, 1570–1575. [[CrossRef](#)]
14. Zhao, R.; Wang, X.; Liu, L.; Li, P.; Tian, L. Slow pyrolysis characteristics of bamboo subfamily evaluated through kinetics and evolved gases analysis. *Bioresour. Technol.* **2019**, *289*. [[CrossRef](#)]
15. da Silva, J.C.G.; Alves, J.L.F.; Galdino, W.V.D.A.; Andersen, S.L.F.; de Sena, R.F. Pyrolysis kinetic evaluation by single-step for waste wood from reforestation. *Waste Manag.* **2018**, *72*. [[CrossRef](#)]
16. Li, X.; Bing, H.; Luo, S.; Zhang, W.; Zuo, Z.; Ren, D. Study on the Pyrolysis Behaviors of Urea-Formaldehyde Resin and Rice Straw Mixed Pellets. *Front. Energy Res.* **2022**, *9*. [[CrossRef](#)]
17. Chen, W.; Chen, Y.; Yang, H.; Xia, M.; Li, K.; Chen, X.; Chen, H. Co-pyrolysis of lignocellulosic biomass and microalgae: Products characteristics and interaction effect. *Bioresour. Technol.* **2017**, *245*. [[CrossRef](#)]
18. Chen, H.; Xie, Y.; Chen, W.; Xia, M.; Li, K.; Chen, Z.; Chen, Y.; Yang, H. Investigation on co-pyrolysis of lignocellulosic biomass and amino acids using TG-FTIR and Py-GC/MS. *Energy Convers. Manag.* **2019**, *196*, 320–329. [[CrossRef](#)]
19. Wongsiriamnuay, T.; Tippayawong, N. Non-isothermal pyrolysis characteristics of giant sensitive plants using thermogravimetric analysis. *Bioresour. Technol.* **2010**, *101*, 5638–5644. [[CrossRef](#)]
20. Feng, Y.S.; Huang, Z.Y.; Mu, J. Pyrolysis characteristics of poplar particleboards containing UF resins. *J. Beijing For. Univ.* **2012**, *34*, 119–122. [[CrossRef](#)]
21. Hirata, T.; Kawamoto, S.; Okuro, A. Pyrolysis of melamine–formaldehyde and urea–formaldehyde resins. *J. Appl. Polym. Sci.* **1991**, *42*. [[CrossRef](#)]
22. Cai, H.; Liu, J.; Xie, W.; Kuo, J.; Buyukada, M.; Evrendilek, F. Pyrolytic kinetics, reaction mechanisms and products of waste tea via TG-FTIR and Py-GC/MS. *Energy Convers. Manag.* **2019**, *184*, 436–447. [[CrossRef](#)]
23. Ding, Y.; Ezekoye, O.A.; Lu, S.; Wang, C. Thermal degradation of beech wood with thermogravimetry/Fourier transform infrared analysis. *Energy Convers. Manag.* **2016**, *120*, 370–377. [[CrossRef](#)]
24. Ferdous, D.; Dalai, A.; Bej, S.; Thring, R.; Bakhshi, N. Production of H₂ and medium Btu gas via pyrolysis of lignins in a fixed-bed reactor. *Fuel Process. Technol.* **2001**, *70*, 9–26. [[CrossRef](#)]
25. Gao, N.; Li, A.; Quan, C.; Du, L.; Duan, Y. TG–FTIR and Py–GC/MS analysis on pyrolysis and combustion of pine sawdust. *J. Anal. Appl. Pyrolysis* **2013**, *100*, 26–32. [[CrossRef](#)]
26. Fang, L.; Liu, L.; Luo, S.; Wang, J.; Zuo, Z.; Peng, B.; Chen, Y.; Yi, C.; Sun, W. Study on the Kinetics and Pyrolysis Behavior of Waste Containing Urea-Formaldehyde Resins. *J. Biobased Mater. Bioenergy J.* **2020**, *14*, 444–452. [[CrossRef](#)]
27. Jiang, X.; Li, C.; Chi, Y.; Yan, J. TG-FTIR study on urea-formaldehyde resin residue during pyrolysis and combustion. *J. Hazard. Mater.* **2010**, *173*, 205–210. [[CrossRef](#)]
28. Richards, G.N. Glycolaldehyde from pyrolysis of cellulose. *J. Anal. Appl. Pyrolysis* **1987**, *10*, 251–255. [[CrossRef](#)]
29. Dong, C.; Zhang, Z.; Liao, H.; Lu, Q. Comparison of Fast Pyrolysis of Poplar and Pine Woods on the Basis of Py-GC-MS Analysis. *Chem. Ind. For. Prod.* **2013**, *33*, 41–47. [[CrossRef](#)]
30. Güllü, D.; Demirbaş, A. Biomass to methanol via pyrolysis process. *Energy Convers. Manag.* **2001**, *42*, 1349–1356. [[CrossRef](#)]
31. Shen, D.; Gu, S. The mechanism for thermal decomposition of cellulose and its main products. *Bioresour. Technol.* **2009**, *100*, 6496–6504. [[CrossRef](#)]
32. Dong, C.-Q.; Zhang, Z.-F.; Lu, Q.; Yang, Y.-P. Characteristics and mechanism study of analytical fast pyrolysis of poplar wood. *Energy Convers. Manag.* **2012**, *57*, 49–59. [[CrossRef](#)]
33. Lu, Q.; Yang, X.-C.; Dong, C.-Q.; Zhang, Z.-F.; Zhang, X.-M.; Zhu, X.-F. Influence of pyrolysis temperature and time on the cellulose fast pyrolysis products: Analytical Py-GC/MS study. *J. Anal. Appl. Pyrolysis* **2011**, *92*, 430–438. [[CrossRef](#)]

34. Piskorz, J.; Radlein, D.; Scott, D.S. On the mechanism of the rapid pyrolysis of cellulose. *J. Anal. Appl. Pyrolysis* **1986**, *9*, 121–137. [[CrossRef](#)]
35. Azeez, A.M.; Meier, D.; Odermatt, J. Temperature dependence of fast pyrolysis volatile products from European and African biomasses. *J. Anal. Appl. Pyrolysis* **2011**, *90*, 81–92. [[CrossRef](#)]

Disclaimer/Publisher’s Note: The statements, opinions and data contained in all publications are solely those of the individual author(s) and contributor(s) and not of MDPI and/or the editor(s). MDPI and/or the editor(s) disclaim responsibility for any injury to people or property resulting from any ideas, methods, instructions or products referred to in the content.